

Article

Proteomic Profiling of Sugar Beet (*Beta vulgaris*) Leaves during Rhizomania Compatible Interactions

Kimberly M. Webb ^{1,*}, Carolyn J. Broccardo ², Jessica E. Prenni ² and William M. Wintermantel ³

¹ USDA-ARS-SBRU, Crops Research Laboratory, 1701 Centre Ave., Fort Collins, CO 80526, USA

² Proteomics and Metabolomics Facility, Colorado State University, C130 Microbiology, 2021 Campus Delivery, Fort Collins, CO 80523, USA; E-Mails:

Carolyn.Broccardo@colostate.edu (C.J.B.); Jessica.Prenni@colostate.edu (J.E.P.)

³ USDA-ARS-CIPRU, 1636 E. Alisal St., Salinas, CA 93905, USA;

E-Mail: Bill.Wintermantel@ars.usda.gov

* Author to whom correspondence should be addressed; E-Mail: Kimberly.webb@ars.usda.gov; Tel.: +1-970-492-7141; Fax: +1-970-492-7160.

Received: 16 January 2014; in revised form: 15 March 2014 / Accepted: 27 March 2014 /

Published: 9 April 2014

Abstract: Rhizomania, caused by *Beet necrotic yellow vein virus* (BNYVV), severely impacts sugar beet (*Beta vulgaris*) production throughout the world, and is widely prevalent in most production regions. Initial efforts to characterize proteome changes focused primarily on identifying putative host factors that elicit resistant interactions with BNYVV, but as resistance breaking strains become more prevalent, effective disease control strategies will require the application of novel methods based on better understanding of disease susceptibility and symptom development. Herein, proteomic profiling was conducted on susceptible sugar beet, infected with two strains of BNYVV, to clarify the types of proteins prevalent during compatible virus-host plant interactions. Total protein was extracted from sugar beet leaf tissue infected with BNYVV, quantified, and analyzed by mass spectrometry. A total of 203 proteins were confidently identified, with a predominance of proteins associated with photosynthesis and energy, metabolism, and response to stimulus. Many proteins identified in this study are typically associated with systemic acquired resistance and general plant defense responses. These results expand on relatively limited proteomic data available for sugar beet and provide the ground work for additional studies focused on understanding the interaction of BNYVV with sugar beet.

Keywords: *Beet necrotic yellow vein virus* (BNYVV); shot-gun proteomics; sugarbeet

1. Introduction

Rhizomania, a disease that reduces root quality and yield in sugar beet (*Beta vulgaris*) is one of the most widely prevalent and economically important diseases affecting sugar beet production throughout the world [1–3]. Rhizomania is caused by *Beet necrotic yellow vein virus* (BNYVV) [4,5] and is transmitted via the plasmodiophorid *Polymyxa betae* [6]. Fields can remain infested with BNYVV indefinitely as *P. betae* cystosori can remain dormant for up to 25 years [4,7]. Therefore, typical remediation approaches such as rotation to non-host crops or lengthening rotations are ineffective at reducing disease incidence, leaving host-plant resistance as the only economically viable means of control [3].

A number of single dominant resistance genes (known as *Rz* genes) have been identified for control of BNYVV beginning with the discovery and introgression of the *Rz1* resistance gene [8,9], which became widely planted throughout all areas where rhizomania threatens sugar beet production. Over the past two decades additional resistance genes have also been identified [10,11]. The different sources of resistance genes appear to have different underlying mechanisms, which are largely undetermined [1,12,13] and several uncharacterized minor genes may contribute to enhanced resistance associated with the primary *Rz* genes [1]. Although the widely used *Rz1* gene prevents symptom development, the virus can still replicate at a low level in resistant plants. This has resulted in emergence of BNYVV variants that can accumulate enough in the presence of the resistance gene and overcome *Rz1* resistance in the field.

Following the introduction of resistant sugar beet varieties containing the single dominant *Rz1* gene, new pathotypes that overcome resistance emerged after only a few cropping seasons [5]. Three major BNYVV types have been reported world-wide; A-type, B-type, and P-type [14–16], with the A-type distributed throughout most sugar beet growing regions of the world [17]. The B-type is predominantly restricted to France and England [16] although limited identifications of the B-type have occurred in Sweden, China, Japan and Iran (summarized in [3]). The A and B types of BNYVV each contain 4 viral RNAs, with RNAs 1 and 2 encoding proteins involved in viral replication, and encapsidation and cell-to-cell movement, respectively. RNA3 encodes a protein that affects pathogenicity and determines the ability of the virus to overcome the most common source of genetic resistance to the virus. RNA4 encodes a single protein involved in transmission by *P. betae* (reviewed in [18]). The P-type is closely related to the A-type, but contains a fifth RNA [17,19]. Isolates containing a fifth RNA usually have increased symptom severity [20]. More importantly, the P-type is able to overcome the *Rz1* resistance gene, which is used to control BNYVV throughout the world. To date the P-type has been restricted to portions of France, Kazakhstan, England, and Iran [15,21–23]. All American isolates identified to date have been A-type, and until a decade ago these were effectively controlled by varieties carrying the *Rz1* gene [8]. In 2002 and 2003, resistant sugar beet in the Imperial Valley of California carrying the *Rz1* resistance gene developed severe rhizomania symptoms due to emergence of a mutant variant of the A-type, now known as the Imperial Strain (BNYVV-IV), which contains

two amino acid mutations in the P25 protein encoded by RNA3 that allow the virus to overcome *Rz1* sources of resistance [5]. Subsequent studies have identified similar resistance-breaking variants throughout American sugar beet production regions, although most are limited in distribution [24]. Little is known of the interactions between sugar beet and BNYVV that influence epidemiology, and until the various mechanisms of resistance and infection are understood more fully, alternative disease control methods and additional sources of resistance will be required to control this pathogen.

There have been some proteomic analyses in sugar beet that have focused on abiotic agronomic stress conditions such as drought [25], salt stress [26,27], and nutritional deficiencies [28], and some examined tissue specific differences in protein expression [29,30]. Few published accounts focused primarily on characterizing the interaction of sugar beet with plant pathogens [31,32]. Proteomic approaches to characterize the interaction of BNYVV with sugar beet have been relatively limited. For example, using a subtractive proteomic approach, Larson *et al.* [32] previously identified 50 putative sugar beet proteins that were either up or down regulated in response to infection with a single BNYVV type. These 50 proteins were uniquely expressed in infected plants of a single susceptible genotype at six weeks after planting compared with uninoculated controls. While Larson *et al.* [32] was able to report on proteins that were differentially expressed with a single BNYVV type, due to the lack of a fully sequenced and annotated sugar beet genome and limitations in the ability to detect low abundance proteins in that study, further analysis of the sugar beet proteome was warranted. The goal of this work is to develop methods for exploratory proteomic profiling of susceptible sugar beet leaves. This approach allows for the unbiased evaluation of the detectable proteins in a sample, and lays the groundwork for future quantitative studies between defined treatments. Such an approach provides data for hypothesis generation and serves to better define the hereto poorly annotated sugar beet proteome. We examined the protein expression during compatible (susceptible) interactions with A-type as well as during infection by the Imperial Strain of BNYVV, which overcomes the *Rz1* resistance gene, the most widely used source of resistance to BNYVV in commercial sugar beet germplasm. This was done in order to identify proteins that are expressed during disease development, in the hopes of gaining an understanding of the proteins that may be involved in the underlying plant defense response.

2. Experimental

2.1. Plant Propagation and Inoculation

A proprietary sugar beet variety, R30_rz1, which is susceptible to all forms of BNYVV, was provided by KWS (Einbeck, Germany). To enable detection of a broad range of proteins associated with compatible interactions, two sources of BNYVV were used; standard BNYVV A-type, originally collected from Spence Field at the USDA-ARS in Salinas, CA (BNYVV-A), and a *Rz1* resistance-breaking mutant variant of the A-type originating from the field, Rockwood 158, Imperial County, CA (BNYVV-IV) [5]. Previous studies indicate that these isolates are virtually identical, differing only by two amino acids in the P25 protein, which allow BNYVV-IV to overcome resistance encoded by the *Rz1* gene [2]. Both isolates are well-characterized and represent the broadest known range of variability expected for North American BNYVV isolates in sugar beet with respect to

performance against the widely planted *Rz1* source of resistance to BNYVV. Soil containing either BNYVV-A or BNYVV-IV was mixed with equal parts sterile builders sand, placed in new Styrofoam cups, and 100 R30_rz1 sugar beet seeds were planted per cup, with five cups per treatment. Seedlings were grown as described in Larson *et al.* [32] in a Conviron PGC15 Growth Chamber (Winnipeg, MB, Canada) at 24 °C with 16 h days and approximately 220 $\mu\text{M m}^{-1}\text{s}^{-2}$ light. At 3 weeks post-germination plants were harvested and washed to remove soil. Seedlings from all five cups for each treatment were pooled, and foliar and root portions of the plant were separated at the crown. Pooled root samples from each treatment were tested by ELISA to confirm BNYVV infection [33]. Only samples with ELISA absorbance readings of at least 2 times the absorbance of healthy controls were subjected to proteomic analysis. Pooled leaf tissue from each treatment was ground in liquid nitrogen and lyophilized. The entire experiment was biologically replicated three times.

2.2. Protein Digestion and Mass Spectrometry

Total protein was extracted from 100 mg (dry weight) of lyophilized leaf tissue for each treatment from each biological replicate, using the Plant Total Protein Extraction Kit (Sigma, St. Louis, MO, USA) according to manufacturer's recommendations. Following extraction, suspended protein was further cleaned for quantification using the ReadyPrep 2-D Cleanup Kit (Bio-Rad, Hercules, CA, USA) in aliquots of 100 μL following manufacturer's recommendations. Protease inhibitors were added to liquid protein extracts (Pierce, Rockford, IL, USA), and samples were stored at $-80\text{ }^{\circ}\text{C}$ prior to analysis. Protein concentrations were determined via Bradford Assay [34] (Thermo Scientific, Rockford, IL, USA) and 30 μg of each sample underwent in-solution proteolytic digestion as previously described [35]. Briefly, samples were solubilized in 8 M urea, 0.2% Protease Max (Promega, Madison, WI, USA), then reduced with dithiothreitol, alkylated with iodoacetamide, and digested with 1% Protease Max and trypsin at 37 °C for 3 h. Samples were dried in a Speed Vac[®] vacuum centrifuge, desalted using Pierce PepClean C18 spin columns (Pierce, Rockford, IL, USA), dried and resuspended in 30 μL 3% ACN, 0.1% formic acid. All solvents, water, and acid were LC-MS/MS grade from Sigma (St. Louis, MO, USA). One μL of each sample (from the three biological replicates from each soil type) was analyzed in duplicate injections via LC-MS/MS. Peptides were purified and concentrated using an on-line enrichment column (Thermo Scientific 5 μm , 100 μm ID \times 2 cm C18 columns). Subsequent chromatographic separation was performed on a reverse phase nanospray column (Thermo Scientific EASYnano-LC, 3 μm , 75 μm ID \times 100 mm C18 column) using a 90 min linear gradient from 10%–30% buffer B (100% ACN, 0.1% formic acid) at a flow rate of 400 nL/min. Peptides were eluted directly into the mass spectrometer (Thermo Scientific Orbitrap Velos Pro) and spectra collected over a m/z range of 400–2,000 Da using a dynamic exclusion limit of 2 MS/MS spectra of a given peptide mass for 30 s (exclusion duration of 90 s). High resolution MS level scans were collected in the FT (resolution of 60,000), and MS/MS spectra were collected in the ion trap (IT). Compound lists of the resulting spectra were generated using Xcalibur 2.2 software (Thermo Scientific, Rockford, IL, USA) with an S/N threshold of 1.5 and 1 scan/group.

2.3. Protein Identification and Data Analysis

MS/MS spectra were searched against a Uniprot *Amaranthaceae* database [36] concatenated to a reverse database and the Uniprot *Mus musculus* (mouse) database [37] using the Mascot database search engine (Matrix Science, version 2.3.2) and SEQUEST (version v.27, rev. 11, Sorcerer, Sage-N Research). Due to the limited size of the *Amaranthaceae* database, the *Mus musculus* sequences were added to ensure adequate database size for statistical scoring and calculation of false discovery rates (FDR) [38]. *Mus musculus* was chosen in order to avoid potential redundant homologous hits with a plant database and any mouse hits were thus ignored in data analysis. While there are EST databases available for *Beta vulgaris* [39,40], we found that there is no straightforward tool to convert the entire database/sequence information to a protein FASTA database. Due to additional complexities associated with assigning the intron/exon sites, start/stop codons, and a lack of meaningful protein annotation from these RNA databases we concluded that conversion would not be an accurate or effective way to identify putative proteins. The following search parameters were used in Mascot: monoisotopic mass, parent mass tolerance of 20 ppm, fragment ion mass tolerance of 0.8 Da, complete tryptic digestion allowing two missed cleavages, variable modification of methionine oxidation, and a fixed modification of cysteine carbamidomethylation. SEQUEST search parameters were the same except for a fragment ion mass tolerance of 1.0 Da and a parent ion tolerance of 0.0120 Da. Peptide identifications from both of the search engines were combined using probabilistic protein identification algorithms in Scaffold version 4.0.3 (Proteome Software, Portland, OR, USA) [41,42] with protein clustering enabled. All data files for each biological replicate were then combined using the “mudpit” option in Scaffold4 generating a composite listing for all proteins identified. Thresholds were set to 99% protein probability, 95% peptide probability, and a 2 unique peptide minimum was required. Peptides shared across proteins were apportioned between proteins according to a weighting function. The peptide FDR was 0% after manual validation of a subset of proteins identified by 2 unique peptides [43]. Criteria for manual validation included the following: (1) a minimum of at least 5 theoretical y or b ions in consecutive order that are peaks greater than 5% of the maximum intensity; (2) an absence of prominent unassigned peaks greater than 5% of the maximum intensity; and (3) indicative residue specific fragmentation, such as intense ions N-terminal to proline and immediately C-terminal to aspartate and glutamate. GO terms were then mapped by Scaffold4 using Uniprot and confirmed manually by literature review. All mass spectrometry data has been deposited to the ProteomeXchange [44] with identifier PXD000237.

2.4. Statistical Analyses for Differentially Expressed Proteins

Unweighted spectrum counts (SpC) and normalized quantitative value for total spectra and average total ion current (TIC) were exported from Scaffold4. *T*-tests were performed in Excel using the normalized quantitative value (for SpC and Avg TIC). Fold change was analyzed using the normalized quantitative value “plus 1” in Excel. Box plots were visualized in DanteR (Pacific Northwest National Laboratories) to assess the effect of normalization on the median spectral counts of each sample. Venn diagrams were generated in Scaffold4.

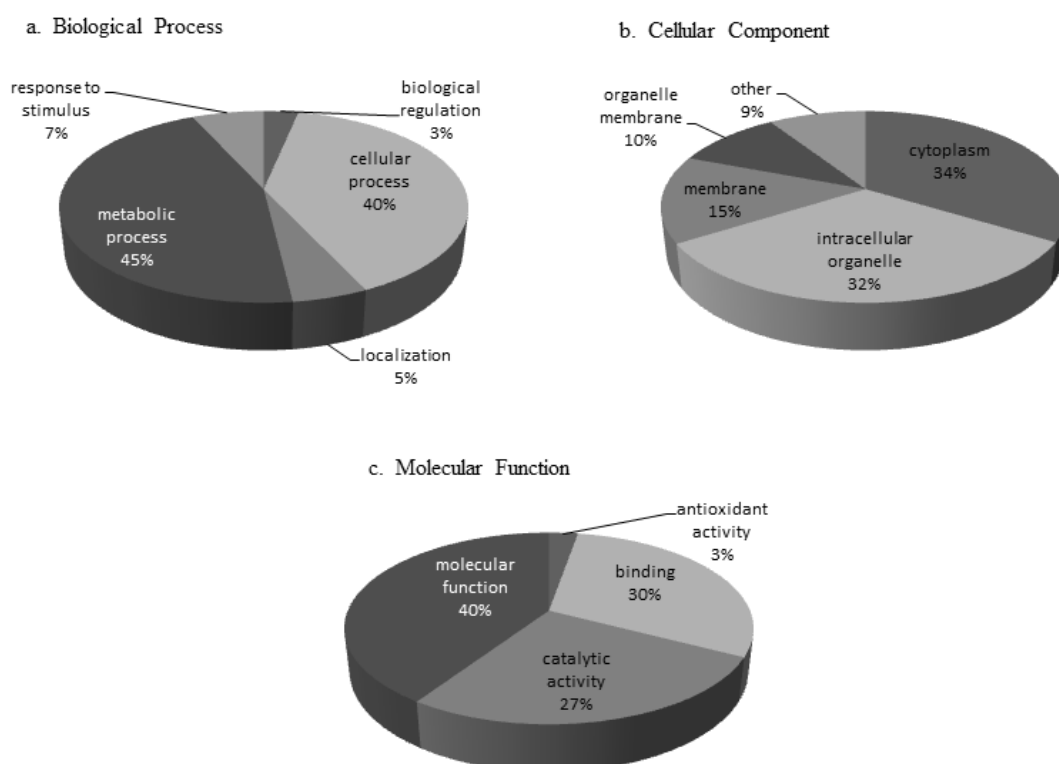
3. Results and Discussion

3.1. Protein Characterization

Prior to protein analysis the presence of BNYVV in test samples was confirmed by performing a BNYVV-specific ELISA assay on all pooled material. ELISA confirmed infection of the susceptible sugar beet variety by both BNYVV pathotypes, with a mean O.D. at 405 nm of 0.382 for BNYVV-IV, and 0.298 for BNYVV-A. Positive samples are considered those with O.D. values of at least twice that of healthy sugar beet (mean O.D. 0.145). Protein assignment was completed using Mascot analysis software and the Uniprot *Amaranthaceae* database with the accession number for each identified protein arranged by predicted annotated function (Supplementary Table S1). A total of 203 proteins (Supplementary Table S1) were identified that met our criteria as defined in the methodology, and mass spectrometry data has been deposited to the ProteomeXchange consortium [44] via the PRIDE partner repository [45] with the dataset identifier PXD000237. Normalized spectral abundance factors (NSAF) were calculated [46] ($NSAF = (\text{unweighted spectrum count}/\text{molecular weight})/\text{sum spectral counts for experiment}$). The 203 proteins were categorized based on annotated GO terms for those proteins that had terms assigned within the categories biological process, cellular component, and molecular function (Figure 1). Categories with increased representation classified under biological process were predicted to function in metabolic (45%) and cellular processes (40%). The predominant protein classes under cellular components in leaf tissue were associated with cytoplasm (34%) and intracellular organelles (32%), while most proteins assigned under the molecular function category were classified as associated with molecular function (40%) and binding (30%) (Figure 1). The majority of the proteins found in the susceptible sugar variety were present during infection by both BNYVV pathotypes. However, there were unique proteins found in interactions with the standard A-type strain (BNYVV-A) that were not found in the resistance breaking strain (BNYVV-IV) and vice versa (Figure 2, Supplementary Table S1). Additionally, the total number of proteins in each predicted annotated function differed during each interaction. For example, there were more putative photosynthesis/energy production and metabolism proteins identified during the interaction with BNYVV-A than during interaction with the resistance breaking strain (BNYVV-IV). In contrast, more signal transduction and transport proteins were identified during the interaction with BNYVV-IV (Figure 2). This suggests that even in compatible interactions, different biological pathways are being induced to create a susceptible interaction in sugar beet dependent on the virus pathotype in question. In a previous study, Larson *et al.* [32] identified 50 proteins that were differentially up or down regulated in individual susceptible and resistant isogenic lines of sugar beet in response to BNYVV infection. In that study, the authors utilized a subtractive proteomic approach in which proteins were separated using a ProteomeLab PF2D, two-dimensional protein fractionation system (Beckman Coulter, Fullerton, CA, USA) and proteins were identified by MALDI-TOF/TOF mass spectrometry. Such an approach required a large amount of protein (>2 mg) in order to detect differential protein peaks for the subtractive analysis and therefore only those proteins with large differences and significant amounts of protein could be detected. In contrast, an untargeted, global proteomic profiling approach was used in our study, which allowed profiling of all detectable proteins, even those at low concentrations. This approach also allowed for the profiling of proteins expressed during compatible

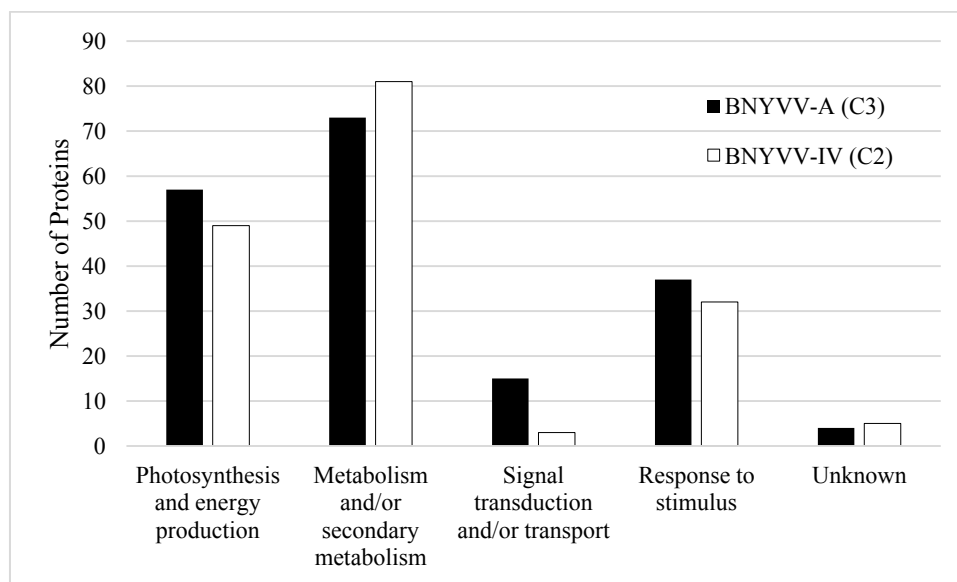
interactions with two pathotypes of BNYVV in a susceptible genotype. This global approach is critical, as it is important to understand all the potential metabolic pathways that may be induced during the response of sugar beet to pathogen infection and perhaps highlight the underlying plant defense response even in susceptible varieties, particularly because so little proteomic data is available for sugar beet. Importantly, this global LC-MS/MS approach is a significant improvement over the use of traditional 2D gels, allowing for easier sample preparation, method development, quantitation, and identification. Despite the difference in methodology, several proteins were identified in the present study that were also found by Larson *et al.* [32] (Supplementary Table S1) including glutamine synthetase, 50S ribosomal proteins, actin 1, profiling, and calmodulin, as well as several putative defense related proteins (superoxide dismutase, ascorbate peroxidase, peroxidases, and chitinase).

Figure 1. Gene Ontology (GO) terms for proteins identified from BNYVV infection of susceptible *Beta vulgaris* leaves. GO terms were collected by Scaffold4 from Uniprot and organized by (a) Biological Process (b) Cellular Component and (c) Molecular Function. Categories are represented as a percent of total identified GO terms.



Many photosynthesis and energy related proteins were found to be expressed during compatible BNYVV interactions in sugar beet, including Ribulose bisphosphate(s), Chlorophyll a/b-binding proteins, photosystem reaction center subunits, ATPase(s), *etc.* (Supplementary Table S1). Management of energy resources by plants during periods of stress commonly occurs in order to provide the necessary energy required to mount a defense, and in some compatible virus/host interactions it is predicted that proteins involved in photosynthesis are likely activated by the virus itself, in order to produce the metabolic energy needed for viral replication (reviewed in [47]).

Figure 2. Total number of proteins identified from susceptible (R30_rz1) *Beta vulgaris* leaves during infection with the standard A-type (BNYVV-A) and the *Rz1* resistance-breaking strain (BNYVV-IV). Proteins are assigned to protein classes based on predicted annotated function as assigned by Scaffold4 using Uniprot and confirmed manually by literature review.



Primary metabolism in plants comprises all metabolic pathways that are essential to the plant's survival, growth, and development. In contrast, secondary metabolites are compounds produced in other metabolic pathways that, although important, are not essential to the functioning of the plant; however, many of these proteins are important in plant defense. Many proteins identified in this study have been associated with primary and secondary metabolic processes in plants (Supplementary Table S1), including glutamine synthetase (B2CZA8) and carbonic anhydrase (P16016).

Signal transduction pathways, which transmit information within individual cells and throughout the plant, are activated whenever biotic and abiotic stresses are recognized at the cellular level, leading to changes in many pathways and cellular processes in plants. Several proteins were expressed during BNYVV infection that are predicted to be associated with signal transduction and transport including three proteins previously reported by Larson *et al.* [32] (Supplementary Table S1). One such protein, calmodulin, has been extensively studied and shown to play crucial role(s) in cellular signaling and regulation of numerous target proteins in plants (reviewed in [48]).

3.2. Response to Stimulus (Including Plant Defense Response) Proteins

Several proteins identified were of primary interest as they had been previously reported to be associated with plant defense responses or responses to other stimuli in plants. Some of these proteins include: glucan endo-1,3- β -D-glucosidase, a 14-3-3 like protein, a pathogenesis related protein, multiple peroxidases, and superoxide dismutase (Supplementary Table S1).

The glucan endo-1,3- β -D-glucosidase (Q9XFW8) is of particular interest. Proteins in this class have been implicated in the hydrolysis of 1,3- β -D-glucosidic linkages in 1,3- β -D-glucans [49] and may contribute to susceptibility of plants to viruses. In plants, callose (a 1,3- β -D-glucan [50,51]) is

deposited between the plasma membrane and the cell wall during the hypersensitive response to infection by both fungi and viruses [49,52]. It is believed that callose acts as a physical barrier limiting the spread of pathogens in resistant plants [53]. It was previously shown that down-regulation of another closely related protein β -1,3-glucanase, contributes to restricting the cell-to-cell movement of TMV, reduced plasmodesmatal size exclusion limits, and enhanced callose deposition in plants [49,54]. How glucan endo-1,3- β -D-glucosidase (Q9XFW8) is “behaving” during the susceptible interaction of BNYVV with sugar beet is unknown, but its identification in this study opens up intriguing avenues of future research to characterize compatible BNYVV/sugar beet interactions.

Another protein of interest was identified as a putative 14-3-3-like protein (P29308). 14-3-3 proteins have been reported to bind other proteins in order to regulate their function in complex environmental signaling pathways and have long been thought to play a role in plant defenses against pathogens. A number of studies implicate some 14-3-3 proteins in R-gene mediated plant disease resistance (reviewed in [55,56]).

During pathogen infection various proteins are induced in association with development of systemic acquired resistance (SAR). These are collectively referred to as pathogenesis-related (PR) proteins. PR proteins are defined as host proteins that are induced by the plant after pathogen attack [57]. We only found a single PR protein (Pathogenesis-related protein 1a/B5QTD3) that was expressed during BNYVV compatible interactions, suggesting that although SAR may be induced in the compatible virus-host interactions, the host response may be limited. However, the specific nature and function of putative PR-1 protein family members is unclear and indicates that this generalized defense response should be evaluated further in subsequent studies.

Three peroxidases were found to be expressed in compatible BNYVV interactions: ascorbate peroxidase (Q42459), and two peroxidases (P93552 and P93547). Peroxidases have been reported to play roles in plant defense to pathogens as a means of protection against the increased production of reactive oxygen species during the hypersensitive response and systemic acquired resistance pathways [58–60]. These have been correlated with accumulation of key enzymes important for building plant cell walls in resistant plants [58]. How putative peroxidases are being utilized in sugar beet during compatible interactions is unknown but they could be associated with generalized plant defense responses to BNYVV infection.

Superoxide dismutases are metalloenzymes found in plants and other organisms that protect cells against super-oxide radicals and prevent formation of other active species of oxygen. During the plant defense response superoxide dismutase expression increases, leading to generation of hydrogen peroxide and increased tolerance to pathogens [61,62]. Up-regulation of superoxide dismutase is believed to contribute in preventing oxidative damage in plants under stress [61,62]. A superoxide dismutase (A7WTB6) was expressed in both compatible BNYVV reactions in the susceptible sugar beet variety lending substantial support to the activity of this enzyme during BNYVV infection; how this protein is contributing to plant defense during compatible interactions should be investigated in future experiments.

3.3. Differential Expression of Proteins during Compatible BNYVV Interactions

During initial proteomic profiling we found that, in general, most of the proteins identified were found during interactions with both BNYVV pathotypes (Figure 2). Using statistical analysis of the unweighted spectrum counts (SpC) and average total ion current (Avg TIC) we found that eight proteins were more highly expressed during infection with the standard A-type strain (BNYVV-A) compared with the resistant breaking strain (BNYVV-IV) (Table 1). All eight proteins were identified in both interactions (Supplementary Table S1) but here we show that some proteins were more highly expressed. The proteins found to be differentially expressed during infection by the standard A-type strain generally fell into the categories metabolism/secondary metabolism and photosynthesis and energy production. Additionally, two proteins were identified that were previously found to be associated with stress responses in plants; a superoxide dismutase and a cytosolic heat shock protein.

Table 1. Proteins differentially expressed in a susceptible sugar beet variety by a standard A-type strain (BNYVV-A) compared to infection by the *Rz1* resistance-breaking strain (BNYVV-IV).

Protein Name	Accession Number	Spectral Counting p -value ($p < 0.1$) ¹	Average TIC p -value ($p < 0.1$) ²
Photosystem II CP43 chlorophyll apoprotein	PSBC_SPIOL	0.025	0.001
Cytosolic heat shock 70 protein	Q41374_SPIOL	0.053	
Superoxide dismutase [Cu-Zn]	H9BQP7_SUASA	0.100	
Glyceraldehyde-3-phosphate dehydrogenase B, chloroplastic	G3PB_SPIOL		0.010
Choline monoxygenase, chloroplastic	CHMO_BETVU		0.032
Fructose-bisphosphate aldolase, chloroplastic	ALFC_SPIOL		0.033
Dehydroascorbate reductase	Q9FVE4_SPIOL		0.061
Formate—tetrahydrofolate ligase	FTHS_SPIOL		0.061

¹ Spectral counting compares the total number of peptide spectra that match to a protein between two groups.

² Average TIC measures the differences in average total ion current off of the mass spectrometer between the two samples.

Pathogen fitness is the ability of the organism to survive and reproduce [63] but can be defined further by using many factors including the level of aggressiveness of the pathogen in susceptible hosts, the ability of the pathogen to survive or persist among a population of other variants or other pathogens, the ability of the pathogen to multiply and spread within the host, as well as having the ability to spread to new hosts ([64], reviewed in [65]). It has been shown that mutations that allow a pathogen to overcome particular resistance genes (*i.e.*, loss of avirulence) also incur a fitness cost to the pathogen during compatible interactions which include decreased aggressiveness (the amount of disease) and reduced symptom expression (reviewed in [65]). Therefore, in susceptible plants, it is possible that the mutation that allows a resistant breaking pathotype to cause disease on resistant hosts, also changes how the pathogen interacts with susceptible hosts and likewise the molecular pathways that are activated in the susceptible host. The finding that there were eight proteins that are more highly expressed in a compatible interaction with the standard A-type BNYVV strain compared with

the resistance breaking strain (BNYVV-IV) suggests that a fitness cost may have been incurred in the resistance breaking strain. Characterization of these mechanisms and their role in pathogen fitness should be more fully elucidated in future experiments.

4. Conclusions

Mass spectrometry based proteomic investigations of non-model systems, such as sugar beet, are challenging due to the lack of a well annotated sequenced genome. Larson *et al.* [32] were only able to identify ~42% of the differentially expressed proteins in that study due to reliance on homology with closely related, fully sequenced organisms when performing database searches for protein identification. A complete genomic sequence for sugar beet was only recently released [66] however it has neither been translated into a protein FASTA database, nor fully annotated. This greatly limits its utility for proteomic applications. The study presented herein represents the first large scale shotgun proteomic analysis of sugar beet, which, combined with homology based database searching against the Uniprot *Amaranthaceae* protein sequence database yielded the confident identification of 203 proteins from BNYVV infected sugar beet. Many proteins identified in susceptible sugar beet during infection with BNYVV were expressed with not just one pathotype, but both. These two BNYVV pathotypes represent the known diversity of BNYVV in the United States (with regards to performance against resistant sources), which justifies future downstream studies to determine specific pathways that may be involved in BNYVV pathogenesis. Understanding how sugar beet responds to infection by BNYVV will enable researchers and producers to identify more effective or novel methods for control of BNYVV infection and rhizomania disease through biotechnology, and may result in improved approaches to manage resistant germplasm, and potentially prolong the functional life of the *Rz* set of resistance genes. The results of this study lay the groundwork for expanded research into the mechanisms and pathways of compatible interactions between BNYVV and sugar beet that lead to development of rhizomania disease. Using the methods established herein, we plan future studies to describe the quantitative differences in protein expression between defined treatment groups. Such a large-scale quantitative approach will be the first of its kind in the field of sugar beet proteomics and should provide critical information on interactions between a virus and disease resistance genes.

Acknowledgments

This work was supported by the Beet Sugar Development Foundation, California Beet Growers Association, Sugarbeet Research and Education Board of Minnesota and North Dakota, and Western Sugar Cooperative-Grower Research Committee. We would like to thank Art Cortez, Paul Covey, Laura Hladky, and Addison Reed for assistance in sample preparation and data collection. We also thank the PRIDE team for assistance with deposit of the mass spectrometry data into the ProteomeXchange database. Mention of trade names or commercial products in this publication is solely for the purpose of providing specific information and does not imply recommendation or endorsement by the U.S. Department of Agriculture. USDA is an equal opportunity provider and employer.

Author Contributions

Conception of experimental design and sugar beet/BNYVV treatment structure was performed by K.M.W. and W.M.W. Sugar beet plant preparations and protein extractions were performed by W.M.W. Protein preparation, mass spectrometry, and sample analysis was performed by C.J.B. and J.E.P. K.M.W. compiled experimental results and had primary responsibility for manuscript preparation with C.J.B., J.E.P. and W.M.W. contributing to manuscript preparation.

Conflicts of Interest

The authors declare no conflict of interest.

References

1. Gidner, S.; Lennefors, B.L.; Nilsson, N.O.; Bensefelt, J.; Johansson, E.; Gyllenspetz, U.; Kraft, T. QTL mapping of BNYVV resistance from the WB41 source in sugar beet. *Genome* **2005**, *48*, 279–285.
2. Rush, C.M.; Liu, H.Y.; Lewellen, R.T.; Acosta-Leal, R. The continuing saga of rhizomania of sugar beets in the United States. *Plant Dis.* **2006**, *90*, 4–15.
3. Pavli, O.I.; Stevanato, P.; Biancardi, E.; Skaracis, G.N. Achievements and prospects in breeding for rhizomania resistance in sugar beet. *Field Crops Res.* **2011**, *122*, 165–172.
4. Abe, H.; Tamada, T. Association of *Beet necrotic yellow vein virus* with isolates of *Polymyxa betae* Keskin. *Ann. Phytopathol. Soc. Jpn.* **1986**, *52*, 235–247.
5. Liu, H.; Sears, J.L.; Lewellen, R.T. Occurrence of resistance breaking *Beet necrotic yellow vein virus* of sugar beet. *Plant Dis.* **2005**, *89*, 464–468.
6. Fujisawa, I.; Sugimoto, T. Transmission of *Beet necrotic yellow vein virus* by *Polymyxa betae*. *Ann. Phytopathol. Soc. Jpn.* **1976**, *43*, 583–586.
7. Tamada, T.; Baba, T. *Beet necrotic yellow vein virus* from rhizomania-affected sugar beet in Japan. *Ann. Phytopathol. Soc. Jpn.* **1973**, *39*, 325–332.
8. Lewellen, R.T.; Skoyen, I.O.; Erichsen, A.W. Breeding sugar beet for resistance to rhizomania: Evaluation of host-plant reactions and selection for and inheritance of resistance. In Proceedings of the 50th Congress of the IIRB, Brussels, Belgium, 11–12 February 1987; pp. 139–156.
9. Lewellen, R.T. Selection for resistance to rhizomania in sugar beet. In Proceedings of the 5th International Congress Plant Pathology, Kyoto, Japan, 20–27 August 1988; p. 455.
10. Scholten, O.E.; Lange, W. Breeding for resistance to rhizomania in sugar beet: A review. *Euphytica* **2000**, *112*, 219–231.
11. Biancardi, E.; Lewellen, R.T.; de Biaggi, M.; Erichsen, A.W.; Stevanato, P. The origin of rhizomania resistance to sugar beet. *Euphytica* **2002**, *127*, 383–397.
12. Scholten, O.E.; Klein-Lankhorst, R.M.; Esselink, D.G.; de Bock, T.S.; Lange, W. Identification and mapping of random amplified polymorphic DNA (RAPD) markers linked to resistance against *Beet necrotic yellow vein virus* (BNYVV) in *Beta* accessions. *Theor. Appl. Genet.* **1997**, *94*, 123–130.

13. Scholten, O.E.; de Bock, T.S.; Klein-Lankhorst, R.M.; Lange, W. Inheritance of resistance to *Beet necrotic yellow vein virus* in *Beta vulgaris* conferred by a second gene for resistance. *Theor. Appl. Genet.* **1999**, *99*, 740–746.
14. Koenig, R.; Luddecke, P.; Kaeberle, A.M. Detection of *Beet necrotic yellow vein virus* strains, variants, and mixed infections by examining single-strand conformation polymorphisms of immunocapture RT-PCR products. *J. Gen. Virol.* **1995**, *76*, 2051–2055.
15. Koenig, R.; Lennefors, B.L. Molecular analyses of European A, B, and P type sources of *Beet necrotic yellow vein virus* and detection of the rare P type in Kazakhstan. *Arch. Virol.* **2000**, *145*, 1561–1570.
16. Kruse, M.; Koenig, R.; Hoffmann, A.; Kaufmann, A.; Commandeur, U.; Solovyev, A.G.; Savenkov, I.; Burgermeister, W. Restriction fragment length polymorphism analysis of reverse transcription PCR products reveals the existence of two major strain groups of *Beet necrotic yellow vein virus*. *J. Gen. Virol.* **1994**, *75*, 1835–1842.
17. Schirmer, A.; Link, D.; Cognat, V.; Moury, B.; Bouve, M.; Meunier, A.; Bragard, C.; Gilmer, D.; Lemaire, O. Phylogenetic analysis of isolates of *Beet necrotic yellow vein virus* collected worldwide. *J. Gen. Virol.* **2005**, *86*, 2897–2911.
18. McGrann, G.R.D.; Grimmer, M.K.; Mutasa-Göttgens, E.S.; Stevens, M. Progress towards the understanding and control of sugarbeet rhizomania disease. *Mol. Plant Pathol.* **2009**, *10*, 129–141.
19. Miyanishi, M.; Kusume, T.; Saito, M.; Tamada, T. Evidence for three groups of sequence variants of beet necrotic yellow vein virus RNA5. *Arch. Virol.* **1999**, *144*, 879–892.
20. Tamada, T.; Kusume, T.; Uchino, H.; Kiguchi, T.; Saito, M. Evidence that *Beet necrotic yellow vein virus* RNA-5 is involved in symptom development of sugarbeet roots. In Proceedings of the Third Symposium of the International Working Group on Plant Viruses with Fungal Vectors, Dundee, UK, 6–7 August 1996; pp. 49–52.
21. Koenig, R.; Kaeberle, A.M.; Commandeur, U. Detection and characterization of resistance-breaking isolates of *Beet necrotic yellow vein virus* in the United States. *Eur. Arch. Virol.* **1997**, *142*, 1499–1504.
22. Ward, L.; Koenig, R.; Budge, G.; Garrido, C.; McGrath, C.; Stubbley, H.; Boonham, N. Occurrence of two different types of RNA-5 containing *Beet necrotic yellow vein virus* in the UK. *Arch. Virol.* **2007**, *152*, 59–73.
23. Mehrvar, M.; Valizadeh, J.; Koenig, R.; Bragard, C. Iranian *Beet necrotic yellow vein virus* (BNYVV): Pronounced diversity of the p25 coding region in A-type BNYVV and identification of P-type BNYVV lacking a fifth RNA species. *Arch. Virol.* **2009**, *154*, 501–506.
24. Liu, H.Y.; Lewellen, R.T. Distribution and molecular characterization of resistance-breaking isolates of *Beet necrotic yellow vein virus* in the United States. *Plant Dis.* **2007**, *91*, 847–851.
25. Hajeidari, M.; Abdollahian-Noghabi, M.; Askari, H.; Heidari, M.; Sadeghian, S.Y.; Ober, E.S.; Salekdeh, G.H. Proteome analysis of sugar beet leaves under drought stress. *Proteomics* **2005**, *5*, 950–960.
26. Wakeel, A.; Asif, A.R.; Pitann, B.; Schubert, S. Proteome analysis of sugar beet (*Beta vulgaris* L.) elucidates constitutive adaptation during the first phase of salt stress. *J. Plant Physiol.* **2011**, *168*, 519–526.

27. Yang, L.; Zhang, Y.; Zhu, N.; Koh, J.; Ma, C.; Pan, Y.; Yu, B.; Chen, S.; Li, H. Proteomic analysis of salt tolerance in sugar beet monosomic addition line M14. *J. Proteome Res.* **2013**, *12*, 4931–4920.
28. Rellan-Alvarez, R.; Andaluz, S.; Rodriguez-Celma, J.; Wohlgemuth, G.; Zocchi, G.; Alvarez-Fernandez, A.; Fiehn, O.; Lopez-Millan, A.F.; Abadia, J. Changes in the proteomic and metabolomic profiles of *Beta vulgaris* root tips in response to iron deficiency and resupply. *BMC Plant Biol.* **2010**, *10*, e120.
29. Catusse, J.; Strub, J.; Job, C.; van Dorsselaer, A.; Job, D. Proteome-wide characterization of sugarbeet seed vigor and its tissue specific expression. *Proc. Natl. Acad. Sci. USA* **2008**, *105*, 10262–10267.
30. Catusse, J.; Meinhard, J.; Job, C.; Strub, J.; Fischer, U.; Pestsova, E.; Westhoff, P.; van Dorsselaer, A.; Job, D. Proteomics reveals potential biomarkers of seed vigor in sugarbeet. *Proteomics* **2011**, *11*, 1569–1580.
31. Larson, R.L.; Hill, A.L.; Nunez, A. Characterization of protein changes associated with sugar beet (*Beta vulgaris*) resistance and susceptibility to *Fusarium oxysporum*. *J. Agric. Food Chem.* **2007**, *55*, 7905–7915.
32. Larson, R.L.; Wintermantel, W.M.; Hill, A.L.; Fortis, L.; Nunez, A. Proteome changes in sugar beet in response to *Beet necrotic yellow vein virus*. *Physiol. Mol. Plant Pathol.* **2008**, *72*, 62–72.
33. Wisler, G.C.; Lewellen, R.T.; Sears, J.L.; Liu, H.; Duffus, J.E. Specificity of TAS-ELISA for *Beet necrotic yellow vein virus* and its application for determining rhizomania resistance in field-grown sugar beets. *Plant Dis.* **1999**, *83*, 864–870.
34. Bradford, M.M. A rapid and sensitive method for the quantification of microgram quantities of protein utilizing the principle of protein-dye binding. *Anal. Biochem.* **1976**, *72*, 248–254.
35. Freund, D.M.; Prenni, J.E.; Curthoys, N.P. Response of the mitochondrial proteome of rat renal proximal convoluted tubules to chronic metabolic acidosis. *Am. J. Physiol.* **2013**, *304*, F145–F155.
36. Uniprot *Amaranthaceae* database. Available online: <http://www.uniprot.org/taxonomy/3563> (accessed on 6 March 2013).
37. Uniprot *Mus musculus* database. Available online: <http://www.uniprot.org/taxonomy/10090> (accessed on 6 March 2013).
38. Giri, P.K.; Kruh, N.A.; Dobos, K.M.; Schorey, J.S. Proteomic analysis identifies highly antigenic proteins in exosomes from *M. tuberculosis*-infected and culture filtrate protein-treated macrophages. *Proteomics* **2010**, *10*, 3190–3202.
39. The Sugarbeet EST database. Available online: http://genomics.msu.edu/cgi-bin/sugarbeet/est_search.cgi (accessed on 5 April 2014).
40. Beta vulgaris Gene Index (BvGI). Available online: http://compbio.dfci.harvard.edu/cgi-bin/tgi/tc_ann.pl?gudb=beet (accessed on 5 April 2014).
41. Keller, A.; Nesvizhskii, A.I.; Kolker, E.; Aebersold, R. Empirical statistical model to estimate the accuracy of peptide identifications made by MS/MS and database search. *Anal. Chem.* **2002**, *74*, 5383–5392.
42. Nesvizhskii, A.I.; Keller, A.; Kolker, E.; Aebersold, R. A statistical model for identifying proteins by tandem mass spectrometry. *Anal. Chem.* **2003**, *75*, 4646–4658.

43. Elias, J.E.; Gygi, S.P. Target-decoy search strategy for increased confidence in large-scale protein identifications by mass spectrometry. *Nat. Methods* **2007**, *4*, 207–214.
44. ProteomeXchange consortium. Available online: <http://proteomecentral.proteomexchange.org> (accessed on 6 March 2013).
45. Vizcaino, J.A.; Cote, R.G.; Csordas, A.; Dianes, J.A.; Fabregat, A.; Foster, J.M.; Griss, J.; Alpi, E.; Birim, M.; Contell, J.; *et al.* The PRoteomics IDentifications (PRIDE) database and associated tools: Status in 2013. *Nucleic Acids Res.* **2013**, *4*, D1063–D1069.
46. Paoletti, A.C.; Parmely, T.J.; Tomomori-Sato, C.; Sato, S.; Zhu, D.; Conaway, R.C.; Conaway, J.W.; Florens, L.; Washburn, M.P. Quantitative proteomic analysis of distinct mammalian mediator complexes using normalized spectral abundance factors. *Proc. Natl. Acad. Sci. USA* **2006**, *103*, 18928–18933.
47. Carli, M.D.; Benvenuto, E.; Donini, M. Recent insights into plant-virus interactions through proteomic analysis. *J. Proteome Res.* **2012**, *11*, 4765–4780.
48. Ranty, B.; Alson, D.; Galaud, J. Plant calmodulins and calmodulin-related proteins. *Plant Signal. Behav.* **2006**, *1*, 96–104.
49. Beffa, R.S.; Hofer, R.M.; Thomas, M.; Meins, F., Jr. Decreased susceptibility to viral disease of [beta]-1,3-glucanase-deficient plants generated by antisense transformation. *Plant Cell* **1996**, *8*, 1001–1011.
50. Bell, A.A. Biochemical mechanisms of disease resistance. *Annu. Rev. Plant Physiol.* **1981**, *32*, 21–81.
51. Stone, B.A.; Clarke, A.E. *Chemistry and Biology of (1-3)-beta-glucans*; La Trobe University Press: Melbourne, Australia, 1992.
52. Aist, J.R. Papillae and related wounds plugs of plant cells. *Annu. Rev. Phytopathol.* **1976**, *14*, 145–163.
53. Allison, A.V.; Shalla, T.A. The ultrastructure of local lesions induced by potato virus X: A sequence of cytological events in the course of infection. *Phytopathology* **1974**, *64*, 784–793.
54. Iglesias, V.A.; Meins, F., Jr. Movement of plant viruses is delayed in a beta-1,3-glucanase deficient mutant showing a reduced plasmodesmatal size exclusion limit and enhanced callose deposition. *Plant J.* **2000**, *21*, 157–166.
55. Roberts, M.R.; Salinas, J.; Collinge, D.B. 14-3-3 proteins and the response to abiotic and biotic stress. *Plant Mol. Biol.* **2002**, *1031*, 1031–1039.
56. Denison, F.C.; Paul, A.L.; Zupanska, A.K.; Ferl, R.J. 14-3-3 proteins in plant physiology. *Semin. Cell Dev. Biol.* **2011**, *22*, 720–727.
57. Van Loon, L.C.; van Strien, E.A. The families of pathogenesis-related proteins, their activities, and comparative analysis of PR-1 type proteins. *Physiol. Mol. Plant Pathol.* **1999**, *55*, 85–97.
58. Chittoor, J.M.; Leach, J.E.; White, F.F. Induction of peroxidase during defense against pathogens. In *Pathogenesis-Related Proteins in Plants*; Datta, S.K., Muthukrishnan, S., Eds.; CRC Press: Boca Raton, FL, USA, 1999; pp. 171–193.
59. Kawano, T. Roles of the reactive oxygen species-generating peroxidase reactions in plant defense and growth induction. *Plant Cell Rep.* **2003**, *21*, 829–837.

60. Caverzan, A.; Passaia, G.; Barcellos Rosa, S.; Werner Ribeiro, C.; Lazzarotto, F.; Margis-Pinheiro, M. Plant responses to stresses: Role of ascorbate peroxidase in the antioxidant protection. *Genet. Mol. Biol.* **2012**, *35*, 1011–1019.
61. Gupta, A.S.; Heinen, J.L.; Holaday, A.S.; Burke, J.J.; Allen, R.D. Increased resistance to oxidative stress in transgenic plants that overexpress chloroplastic Cu/Zn superoxide dismutase. *Proc. Natl. Acad. Sci. USA* **1993**, *90*, 1629–1633.
62. Tsang, E.; Bowler, C.; Herouart, D.; van Camp, W.; Villarroel, R.; Genetello, C.; van Montagu, M.; Inze, D. Differential regulation of superoxide dismutases in plants exposed to environmental stress. *Plant Cell* **1991**, *3*, 783–792.
63. Crow, J.F. *Basic Concepts in Population, Quantitative, and Evolutionary Genetics*; Academic Press: New York, NY, USA, 1986; p. 273.
64. Antonovics, J.; Alexander, H.M. The concept of fitness in plant-fungal pathogen systems. In *Plant Disease Epidemiology*; Leonard, K.J., Fry, W.E., Eds.; McGraw-Hill: New York, NY, USA, 1989; pp. 185–214.
65. Leach, J.E.; Vera Cruz, C.M.; Bai, J.; Leung, H. Pathogen fitness penalty as a predictor of durability of disease resistance genes. *Annu. Rev. Phytopathol.* **2001**, *39*, 187–224.
66. Eujayl, I.; Strausbaugh, C. *Beta vulgaris* subsp. *Vulgaris*. Available online: <http://www.ncbi.nlm.nih.gov/Traces/wgs/?val=ARYA01> (accessed on 5 April 2014).

© 2014 by the authors; licensee MDPI, Basel, Switzerland. This article is an open access article distributed under the terms and conditions of the Creative Commons Attribution license (<http://creativecommons.org/licenses/by/3.0/>).

Supplementary Material

Table S1. List of proteins identified in the *Beta vulgaris* leaf proteome during BNYVV infection of susceptible sugar beet via mass spectrometry.

Protein Name ¹	Uniprot Accession	Name	Mass kDa	NSAF ²	Number Unique Peptides	% Coverage	BNYVV-IV (C2) ³	BNYVV-IV (C3) ⁴
Photosynthesis and energy production								
Ribulose biphosphate carboxylase large chain	Q4PLI7	rbcL	53	3.50E-03	88	66%	x	x
ATP synthase subunit beta, chloroplastic	Q4PLI6	atpB	54	1.40E-03	39	85%	x	x
Ribulose biphosphate carboxylase small chain	P00870	RBCS	14	1.00E-03	6	51%	x	x
Rubisco activase	Q8L5T3	rca	48	7.80E-04	25	49%	x	x
ATP synthase subunit alpha, chloroplastic	P06450	atpA	55	6.20E-04	35	47%	x	x
Cytochrome b559 subunit alpha	Q2Z1Q5	psbE	9	4.00E-04	4	48%	x	x
Photosystem I iron-sulfur center	P10098	psaC	9	3.60E-04	8	83%	x	x
Photosystem I reaction center subunit IV, chloroplastic	P12354	PSAE-1	13	3.50E-04	4	35%	x	x
Glyceraldehyde-3-phosphate dehydrogenase B, chloroplastic	P12860	GAPB	48	3.30E-04	10	33%	x	x
Photosystem I reaction center subunit II, chloroplastic	P12353	psaD	23	3.20E-04	9	32%	x	x
Phosphoglycerate kinase, chloroplastic	P29409		46	3.10E-04	16	42%	x	x
Chlorophyll a/b-binding protein	O49812		28	3.10E-04	9	57%	x	x
Phosphoribulokinase, chloroplastic	P09559		45	2.90E-04	5	46%	x	x
Glycine decarboxylase subunit T	Q947L6	gdt	14	2.80E-04	7	78%	x	x
Glyceraldehyde-3-phosphate dehydrogenase A, chloroplastic	P19866	GAPA	43	2.70E-04	8	28%	x	x
Oxygen-evolving enhancer protein 1, chloroplastic	P12359	PSBO	35	2.60E-04	2	25%		x
ATP synthase subunit b, chloroplastic	P06453	atpF	21	2.00E-04	7	38%	x	x
23 kDa OEC protein	B0L802	PsbP	22	1.70E-04	4	15%	x	x

Table S1. Cont.

Protein Name ¹	Uniprot Accession	Name	Mass kDa	NSAF ²	Number Unique Peptides	% Coverage	BNYVV-IV (C2) ³	BNYVV-IV (C3) ⁴
Photosystem I reaction center subunit VI, chloroplastic	P22179	PSAH	15	1.60E-04	2	8.30%	x	x
Dihydrolipoamide dehydrogenase	Q947M1	dhl	18	1.60E-04	6	51%	x	x
V-type proton ATPase catalytic subunit A	Q39442		69	1.60E-04	27	54%	x	x
Chlorophyll a/b binding protein	Q7XAC6	cab11	28	1.40E-04	7	52%	x	x
Sedoheptulose-1,7-bisphosphatase, chloroplastic	O20252		42	1.20E-04	7	19%	x	x
Photosynthetic oxygen-evolving protein 16 kDa subunit	B0L6Y3	psbQ	25	1.20E-04	2	15%	x	x
Apocytochrome f	P16013	petA	35	1.10E-04	7	20%	x	x
Glycine decarboxylase subunit P	Q947L7	gdp	8	1.00E-04	5	40%		x
Photosystem II reaction center protein H	P05146	psbH	8	9.30E-05	2	29%	x	x
Cytochrome b6	P00165	petB	24	9.20E-05	3	21%	x	x
Triosephosphate isomerase, chloroplastic	P48496	TPIP1	34	8.90E-05	6	32%	x	x
Chloroplast ribose-5-phosphate isomerase	Q8RU73		31	8.80E-05	4	16%	x	x
ADP-ribosylation factor 1	H2EP74	ARF1	21	8.50E-05	8	46%	x	x
Fructose-1,6-bisphosphatase, chloroplastic	P22418		45	8.10E-05	4	13%	x	x
ATP-dependent Clp protease proteolytic subunit	Q9M3K5	clpP	22	6.90E-05	2	21%		x
ATP synthase subunit b', chloroplastic	P31853	ATPG	24	6.40E-05	2	9.00%	x	x
ATP synthase epsilon chain, chloroplastic	P00833	atpE	15	5.90E-05	2	16%	x	x
ATP synthase delta chain, chloroplastic	P11402	ATPD	28	5.70E-05	3	7.40%		x
Photosystem I reaction center subunit XI, chloroplastic	Q41385	PSAL	23	5.40E-05	2	12%	x	x

Table S1. Cont.

Protein Name ¹	Uniprot Accession	Name	Mass kDa	NSAF ²	Number Unique Peptides	% Coverage	BNYVV-IV (C2) ³	BNYVV-IV (C3) ⁴
V-type proton ATPase subunit E	Q41396	VATE	26	5.40E-05	9	48%	x	x
Photosystem II 22 kDa protein, chloroplastic	Q02060	PSBS	29	4.70E-05	4	20%	x	x
Photosystem II CP43 chlorophyll apoprotein	Q6EY72	psbC	46	4.60E-05	2	19%	x	x
Photosystem I reaction center subunit V, chloroplastic	P12357	PSAG	18	4.50E-05	3	10%	x	x
Ribulose-phosphate 3-epimerase, chloroplastic	Q43157	RPE	30	4.50E-05	2	15%		x
Photosystem II D2 protein	P06005	psbD	40	4.10E-05	3	9.10%	x	x
Cytochrome b6-f complex iron-sulfur subunit, chloroplastic	P08980	petC	24	4.00E-05	3	17%	x	x
Photosystem II CP43 chlorophyll apoprotein	P06003	psbC	52	3.60E-05	3	25%	x	x
Photosystem I reaction center subunit III, chloroplastic	P12355	PSAF	25	3.50E-05	4	20%	x	x
Photosystem Q(B) protein	P69565	psbA	39	1.90E-05	4	16%	x	x
Delta-aminolevulinic acid dehydratase, chloroplastic	P24493	HEMB	47	1.90E-05	3	18%	x	x
Photosystem I P700 chlorophyll a apoprotein A2	P06512	psaB	82	1.90E-05	5	9.80%	x	x
Oxygen-evolving enhancer protein 3, chloroplastic	P12301	PSBQ	25	1.70E-05	3	5.20%	x	x
Vacuolar proton pump ATPase subunit H	G4XKY2	VHA-H	53	1.50E-05	5	12%	x	x
Violaxanthin de-epoxidase, chloroplastic	Q9SM43	VDE1	54	1.40E-05	3	7.80%	x	x
Type III chlorophyll a/b-binding protein	Q9AVE9	cab3	17	9.90E-06	2	16%		x
NADPH-protochlorophyllide oxidoreductase 2	Q9AVF1	POR2	25	4.80E-06	3	20%		x
UDP-glucose:flavonoid-O-glucosyltransferase	Q5GIG8		54	4.00E-06	2	6.50%	x	

Table S1. Cont.

Protein Name ¹	Uniprot Accession	Name	Mass kDa	NSAF ²	Number Unique Peptides	% Coverage	BNYVV-IV (C2) ³	BNYVV-IV (C3) ⁴
26S protease regulatory subunit 7	Q41365	RPT1	48	2.00E-06	2	6.60%		x
Photosystem I P700 chlorophyll a apoprotein A1	P06511	psaA	83	1.70E-06	2	2.30%		x
Metabolism and/or secondary metabolism								
Glyceraldehyde-3-phosphate dehydrogenase	A3FMH0		37	5.10E-04	19	79%	x	x
Glutamine synthetase	B2CZA8	GNL2	47	4.00E-04	20	56%	x	x
Malate dehydrogenase, cytoplasmic	Q9SML8	NR1	35	3.60E-04	16	64%	x	x
Serine hydroxymethyltransferase	Q947K8	sht	5	2.70E-04	2	32%	x	x
Fructose-bisphosphate aldolase, chloroplastic	P16096		42	2.50E-04	13	32%	x	x
Methionine synthase	Q4H1G2	BvMS1	88	2.30E-04	15	48%	x	x
50S ribosomal protein L12, chloroplastic	Q53WU1	Soc	20	2.30E-04	6	33%	x	x
Alpha tubulin	B5BT09	TUB	24	2.00E-04	6	56%	x	x
S-adenosylmethionine synthase 1	Q4H1G4	SAMS1	43	1.80E-04	22	68%	x	x
Adenosylhomocysteinase	Q4H1G1	BvSAHH1	53	1.70E-04	24	60%	x	x
Transketolase, chloroplastic	O20250		80	1.70E-04	13	21%	x	x
ClpC protease	O98447	clpC	99	1.60E-04	39	51%	x	x
Elongation factor 1-alpha	Q8H9A9	skef-1A	49	1.60E-04	19	38%	x	x
50S ribosomal protein L14, chloroplastic	P09596	rpl14	13	1.30E-04	5	51%	x	x
Carbonic anhydrase, chloroplastic	P16016		35	1.10E-04	3	13%	x	x
Elongation factor 2	O23755		94	1.10E-04	28	50%	x	x
Sal k 3 pollen allergen	C1KEU0		84	1.10E-04	2	22%	x	x
Choline monooxygenase, chloroplastic	O22553	CMO	50	1.00E-04	12	33%	x	x
Elongation factor 1-delta	O81918		25	1.00E-04	5	40%	x	x
Glutamate synthase	I6PD11		157	9.60E-05	46	42%	x	x
Carbonic anhydrase	Q947M3		14	9.30E-05	2	20%		x
30S ribosomal protein S17, chloroplastic	P82137	RPS17	4	9.00E-05	2	47%		x
Enolase	Q9LEE0	eno	48	8.40E-05	9	29%	x	x
Fructose-bisphosphate aldolase	Q6RSN7		39	7.10E-05	6	25%	x	x

Table S1. Cont.

Protein Name ¹	Uniprot Accession	Name	Mass kDa	NSAF ²	Number Unique Peptides	% Coverage	BNYVV-IV (C2) ³	BNYVV-IV (C3) ⁴
Glutamate 1-semialdehyde aminotransferase	Q9AVF5	GSA-AT	33	7.10E-05	6	23%	x	x
Glucose-1-phosphate adenylyltransferase small subunit, chloroplastic/amyloplastic	P55232	AGPB1	54	6.60E-05	15	43%	x	x
30S ribosomal protein S11, chloroplastic	P06506	rps11	15	6.60E-05	3	24%	x	x
Pyruvate dehydrogenase E1alpha subunit	Q852S0	PDH E1a-1	44	6.50E-05	8	29%	x	x
30S ribosomal protein S4, chloroplastic	P13788	rps4	23	6.10E-05	8	39%	x	x
50S ribosomal protein L5, chloroplastic	P82192	RPL5	24	6.00E-05	2	12%	x	x
Plasma membrane intrinsic protein PIP1;1	C7DYC4		31	5.80E-05	6	36%	x	x
30S ribosomal protein S16, chloroplastic	P28807	rps16	10	5.80E-05	2	24%	x	x
50S ribosomal protein L2, chloroplastic	P06509	rpl2-A	30	5.60E-05	5	25%	x	x
Nucleoside diphosphate kinase 2, chloroplastic	Q01402	NDPK2	26	5.20E-05	3	15%	x	x
30S ribosomal protein S1, chloroplastic	P29344	RPS1	45	5.10E-05	8	17%	x	x
Fructose-1,6-bisphosphatase, cytosolic	Q42649		37	5.00E-05	3	25%	x	x
Isocitrate dehydrogenase	Q9SPH8	Icdh	28	4.80E-05	3	12%	x	x
Uroporphyrinogen decarboxylase	Q9AVF8	UROD	21	4.70E-05	4	26%	x	x
Proteasome subunit alpha type	I6U5E4	PAC1	27	4.60E-05	2	28%	x	x
Ferredoxin—NADP reductase, chloroplastic	P00455	PETH	41	4.60E-05	4	13%	x	x
Fructokinase	Q42645		35	4.10E-05	10	40%	x	x
Cysteine synthase	B5U9U9	CSase A	34	4.10E-05	4	20%	x	x
Nitrite reductase	E2JFE1	NiR	67	4.00E-05	8	30%	x	x
Glutamine synthetase	B0LSR3	GNL1	39	3.90E-05	6	32%	x	x
Ribosome-recycling factor, chloroplastic	P82231	RRF	30	3.50E-05	4	13%	x	x
Ketol-acid reductoisomerase, chloroplastic	Q01292	AHRI	64	3.50E-05	11	24%	x	x

Table S1. Cont.

Protein Name ¹	Uniprot Accession	Name	Mass kDa	NSAF ²	Number Unique Peptides	% Coverage	BNYVV-IV (C2) ³	BNYVV-IV (C3) ⁴
Fructose-bisphosphate aldolase, cytoplasmic isozyme	P29356		38	3.30E-05	3	9.50%	x	x
Dehydroascorbate reductase	Q9FVE4	DHAR	30	3.30E-05	3	11%	x	x
30S ribosomal protein S13, chloroplastic	P82163	RPS13	16	3.20E-05	2	9.70%	x	x
40S ribosomal protein S25	Q94G66	RPS25	13	2.80E-05	2	21%	x	x
60S acidic ribosomal protein P0	P29764		34	2.70E-05	3	8.70%	x	x
30S ribosomal protein S9, chloroplastic	P82278	PRPS9	21	2.60E-05	3	23%	x	x
Peptidyl-prolyl cis-trans isomerase, chloroplastic	O49939	TLP40	50	2.40E-05	3	10%	x	x
30S ribosomal protein S5, chloroplastic	Q9ST69	rps5	34	2.40E-05	3	13%	x	x
Acyl-[acyl-carrier-protein] desaturase, chloroplastic	P28645		46	2.30E-05	4	13%	x	x
50S ribosomal protein L24, chloroplastic	P27683	RPL24	21	2.30E-05	2	10%	x	
Formate—tetrahydrofolate ligase	P28723		68	2.30E-05	6	14%	x	x
30S ribosomal protein S8, chloroplastic	P09597	rps8	16	2.10E-05	3	22%	x	x
rRNA N-glycosidase	B1VCR4		28	2.00E-05	3	14%	x	x
50S ribosomal protein L1, chloroplastic	Q9LE95	RPL1	39	2.00E-05	2	6.80%	x	x
Phosphoenolpyruvate carboxylase	B2MW80		110	1.90E-05	16	15%	x	x
Phosphoethanolamine N-methyltransferase	Q9M571	PEAMT	56	1.70E-05	4	8.30%		x
Coproporphyrinogen oxidase	Q9AVF7	COPROX	19	1.60E-05	2	12%		x
Sucrose synthase	Q6SJP5	SBSS2	92	1.60E-05	7	16%	x	x
40S ribosomal protein S11	Q1H8R1	rpS11	18	1.60E-05	2	15%	x	x
Fatty acid hydroperoxide lyase	E7E818	HPL	55	1.40E-05	5	13%	x	x
50S ribosomal protein L16, chloroplastic	P17353	rpl16	15	1.10E-05	2	16%	x	x

Table S1. Cont.

Protein Name ¹	Uniprot Accession	Name	Mass kDa	NSAF ²	Number Unique Peptides	% Coverage	BNYVV-IV (C2) ³	BNYVV-IV (C3) ⁴
Granule bound starch synthase I	D6RSA2	GBSSI	67	1.10E-05	3	6.90%	x	
Malate dehydrogenase [NADP], chloroplastic	P52426	MDH	47	1.00E-05	2	6.40%		x
Proteasome subunit beta type-5	O24361		30	9.60E-06	2	8.50%	x	
30S ribosomal protein S19 alpha, chloroplastic	P06508	rps19	11	8.70E-06	2	33%		x
Phosphoserine aminotransferase, chloroplastic	P52877		47	8.70E-06	4	10.00%	x	x
30S ribosomal protein S3, chloroplastic	P09595	rps3	25	8.60E-06	5	23%		x
6-phosphogluconate dehydrogenase, decarboxylating 1	Q94KU1	pgdC	53	6.80E-06	3	12%	x	x
50S ribosomal protein L11, chloroplastic	P31164	rpl11	24	6.00E-06	2	14%	x	x
11S globulin seed storage protein	Q38712		57	5.90E-06	2	4.40%	x	x
Putative vacuolar processing enzyme	Q949L7		54	5.80E-06	3	8.60%	x	
UDP-sulfoquinovose synthase, chloroplastic	Q84KI6	SQD1	54	5.80E-06	2	7.70%	x	x
Delta 1-pyrroline-5-carboxylate synthetase	Q8LRT0	P5CS	24	4.00E-06	2	15%		x
Monodehydroascorbate reductase	Q94IB7		54	4.00E-06	2	6.40%	x	x
Myo-inositol-1-phosphate synthase	Q944C3	INPS	57	3.80E-06	2	6.10%		x
Hexokinase-1	Q9SEK3	HXK1	54	3.60E-06	2	8.00%		x
Cysteine synthase like protein	Q767A2	CSaseLP	36	3.30E-06	2	11%		x
Glucose-6-phosphate isomerase	O82058	GPIP	68	2.80E-06	2	4.00%	x	x
Glycylpeptide N-tetradecanoyltransferase	K4Q1D5		51	1.90E-06	2	7.80%		x
Glucose-1-phosphate adenylyltransferase large subunit, chloroplastic/amyloplastic	P55233	AGPS1	58	1.70E-06	2	4.00%	x	x

Table S1. Cont.

Protein Name ¹	Uniprot Accession	Name	Mass kDa	NSAF ²	Number Unique Peptides	% Coverage	BNYVV-IV (C2) ³	BNYVV-IV (C3) ⁴
Signal transduction and/or transport								
33 kDa protein of the oxygen-evolving complex	B5BT06	OEE1	35	4.70E-04	7	56%	x	x
Non-specific lipid-transfer protein	Q7XZE0	AnLTP	12	4.30E-04	2	11%	x	
Beta-tubulin	A3FMG7		12	3.50E-04	6	60%	x	
Actin 1	E9P160		42	3.50E-04	20	64%	x	
Profilin	A8VT60		14	2.20E-04	3	24%	x	
Calmodulin	Q3UKW2	Calm1	22	1.50E-04	7	73%	x	
Voltage-dependent anion channel protein	Q41368	SVDAC1	30	1.50E-04	7	30%	x	
28 kDa ribonucleoprotein, chloroplastic	P28644		25	1.30E-04	6	30%	x	
Putative GTP binding protein	Q0MX58		23	9.40E-05	7	27%	x	
Luminal-binding protein	Q42434	HSC70	74	5.50E-05	11	26%	x	
Plasma membrane major intrinsic protein 2	Q39440		30	5.00E-05	9	41%	x	
20 kDa chaperonin, chloroplastic	Q02073	CPN21	27	4.80E-05	2	7.10%	x	
Calreticulin	O81919		48	4.00E-05	7	29%	x	
Chloroplast mRNA-binding protein CSP41	O24365		45	2.70E-05	3	6.70%	x	
Protein phosphatase 2A	H6VX93	PP2A	35	8.20E-06	3	21%		x
Protein translocase subunit SecA, chloroplastic	Q36795	secA	117	4.70E-06	2	3.40%		x
Response to stimulus (including plant defense response)								
Peroxisomal (S)-2-hydroxy-acid oxidase	P05414		40	3.40E-04	17	54%	x	x
Cytosolic heat shock 70 protein	O22664	HSC70	71	2.40E-04	25	45%	x	x
Peroxiredoxin Q, chloroplastic	Q6UBI3	PRXQ	24	2.30E-04	8	36%	x	x
Superoxide dismutase [Cu-Zn]	A7WTB6		22	2.20E-04	6	20%	x	x
Heat shock 70 protein	O50036	HSC70-9	76	1.90E-04	24	38%	x	x
Glucan endo-1,3-beta-D-glucosidase	Q9XFW8	Glu2	36	1.50E-04	14	63%	x	x
14-3-3-like protein	P29308		25	1.40E-04	9	28%	x	x
Ascorbate peroxidase	Q42459		28	1.30E-04	3	28%	x	x

Table S1. Cont.

Protein Name ¹	Uniprot Accession	Name	Mass kDa	NSAF ²	Number Unique Peptides	% Coverage	BNYVV-IV (C2) ³	BNYVV-IV (C3) ⁴
Catalase	Q94EV9	CAT1	57	1.30E-04	9	23%	x	x
2-Cys peroxiredoxin BAS1, chloroplastic	O24364	BAS1	29	1.30E-04	5	25%	x	x
Cell wall peroxidase	O81266		9	7.70E-05	2	61%	x	x
Laccase-like protein	I3W7E6		51	7.50E-05	12	36%	x	x
Superoxide dismutase	H9BQP5	MnSOD	26	7.50E-05	4	25%	x	x
Thioredoxin M-type, chloroplastic	P07591		20	7.40E-05	3	10%	x	x
Thaumatin like protein	Q949L8		23	5.70E-05	3	20%	x	x
Peroxidase prx13	Q9M4Z4		36	5.40E-05	3	17%	x	x
Chitinase	Q9XFW7	Ch4	28	5.10E-05	7	44%	x	x
Heat shock protein 83	Q1H8M1	hsp83	40	4.60E-05	7	28%	x	x
Germin-like protein Kiel 1	Q84RC0	GLP-Ki1	22	4.40E-05	3	11%	x	x
Pathogenesis-related protein 1a	B5QTD3	pr1a	18	3.90E-05	3	32%	x	
Germin-like protein Wageningen 1	Q84V63	GLP-Wag1	22	3.50E-05	4	16%	x	
Betaine aldehyde dehydrogenase, chloroplastic	P28237		55	3.40E-05	12	29%	x	x
Salt tolerance protein 4	Q84LL8	sato4	22	2.90E-05	2	16%	x	x
Salt tolerance protein 2	Q711N3	sato2	38	2.70E-05	6	23%	x	x
Major latex like protein homolog	Q949M0		17	2.40E-05	4	27%	x	x
Peroxisomal ascorbate peroxidase	L0CTS4		31	2.30E-05	6	31%	x	x
Peroxidase	P93552	prxr8	36	2.20E-05	3	15%	x	
Catalase	Q941J0	cat2	33	2.00E-05	3	12%	x	x
Heat shock 70 protein	O49045	HSC70-10	72	1.90E-05	5	16%	x	x
Peroxidase	P93547	prxr3	38	1.80E-05	2	11%	x	
Acidic endochitinase SP2	P42820	SP2	30	1.70E-05	5	24%	x	
Salt tolerance protein 5	Q84LL6	sato5	33	1.50E-05	2	17%	x	x
Auxin-induced beta-glucosidase	Q7XJH8		83	1.40E-05	4	8.00%	x	x
Acidic endochitinase SE2	P36910	SE2	31	1.40E-05	2	11%	x	
Cationic peroxidase	Q1H8N1	cprx1	35	1.00E-05	4	25%	x	x
DnaJ protein homolog ANJ1	P43644		47	9.70E-06	2	8.90%	x	x
Chitinase	Q42421	Ch1	48	6.50E-06	3	13%	x	x
Stress-induced protein sti1-like protein	H9B3R7		51	1.40E-06	2	5.10%		x

Table S1. Cont.

Protein Name ¹	Uniprot Accession	Name	Mass kDa	NSAF ²	Number Unique Peptides	% Coverage	BNYVV-IV (C2) ³	BNYVV-IV (C3) ⁴
Unknown or other								
RS2 protein	Q9FNT2	Rs2	16	1.40E-04	7	33%	x	x
Putative uncharacterized protein	E2DN06		15	1.20E-04	2	16%	x	x
Histone H3.3C	P02301	H3f3c	15	9.80E-05	5	51%	x	x
Putative uncharacterized protein	E2DN04		15	3.40E-05	2	13%	x	
37 kDa inner envelope membrane protein, chloroplastic	P23525		39	1.70E-05	3	14%		x
Uncharacterized protein	K4PYU2		18	8.00E-06	2	13%		x

Footnotes: ¹ Proteins are organized based on GO terms and putative annotated function. ² NSAF: Normalized spectral abundance factors. ³ C2: Proteins that were identified from the susceptible sugar beet genotype (R30_rz1) infected with the resistance breaking BNYVV strain from the Rockwood 158 field, Imperial County, CA (BNYVV-IV). ⁴ C3: Proteins that were identified from the susceptible sugar beet genotype (R30_rz1) infected with A-type of BNYVV (BNYVV-A) strain. Proteins in **bold** lettering were previously identified in the study by Larson *et al.* [1].

References

1. Larson, R.L.; Hill, A.L.; Nunez, A. Characterization of protein changes associated with sugar beet (*Beta vulgaris*) resistance and susceptibility to *Fusarium oxysporum*. *J. Agric. Food Chem.* **2007**, *55*, 7905–7915.

© 2014 by the authors; licensee MDPI, Basel, Switzerland. This article is an open access article distributed under the terms and conditions of the Creative Commons Attribution license (<http://creativecommons.org/licenses/by/3.0/>).